

Regulation by small RNAs via coupled degradation: mean-field and variational approaches

Thierry Platini*

*Virginia Bioinformatics Institute,
Virginia Polytechnic Institute and State University,
Blacksburg, VA 24061, USA*

Tao Jia[†] and Rahul V. Kulkarni[‡]

*Department of Physics,
Virginia Polytechnic Institute and State University,
Blacksburg, VA 24061, USA*

(Dated: November 27, 2021)

Regulatory genes called small RNAs (sRNAs) are known to play critical roles in cellular responses to changing environments. For several sRNAs, regulation is effected by coupled stoichiometric degradation with messenger RNAs (mRNAs). The nonlinearity inherent in this regulatory scheme indicates that exact analytical solutions for the corresponding stochastic models are intractable. Here, we present a variational approach to analyze a well-studied stochastic model for regulation by sRNAs via coupled degradation. The proposed approach is efficient and provides accurate estimates of mean mRNA levels as well as higher order terms. Results from the variational ansatz are in excellent agreement with data from stochastic simulations for a wide range of parameters, including regions of parameter space where mean-field approaches break down. The proposed approach can be applied to quantitatively model stochastic gene expression in complex regulatory networks.

PACS numbers: 87.10.Mn, 02.50.r, 82.39.Rt, 87.17.Aa, 45.10.Db

A new paradigm for cellular regulation has emerged in recent years with the discovery of novel non-coding genes called small RNAs (sRNAs). In bacteria, sRNAs often function as global regulators that mediate cellular adaptation to changing environments [1]. In higher organisms, the corresponding genes (microRNAs) are known to play key roles in the regulation of critical processes such as development, stem cell pluripotency and cancer [2, 3]. It has been proposed that one of the key functions of sRNAs in controlling cellular processes is to regulate the variability (noise) in gene expression [3]. Recent experimental developments have led to approaches for quantifying such variability using single-molecule measurements of mRNA levels [4]. These technological advances have now made possible experimental studies that analyze the roles of sRNAs in noise regulation during important processes such as development. Correspondingly, there is a need for theoretical approaches that complement such experimental efforts to enable a quantitative understanding of different mechanisms of sRNA-based regulation.

While the molecular mechanisms of sRNA-mediated regulation continue to be investigated, one established mechanism, representative of several bacterial sRNAs, corresponds to binding with mRNAs followed by coupled stoichiometric degradation [5]. An important challenge for current research is to analyze how this regulatory mechanism impacts the variability of gene expression across a population of cells. Several recent theoretical studies [6–11] have analyzed models based on the corresponding reaction scheme (shown in Fig. 1A). The nonlinearity inherent in this reaction scheme im-

plies that exact analytical solutions for the corresponding stochastic model are intractable; thus approximate analytical approaches are needed. Previous theoretical studies have primarily focused on mean-field (MF) approaches and on steady-state distributions using expansions around MF solutions. However, MF approaches are not accurate when we have a combination of nonlinear reaction rates (due to interaction with small RNAs) and low mRNA/sRNA levels, which points to the need for development of alternative analytical approaches.

In this paper, we analyze stochastic models of sRNA-based regulation via coupled degradation (as shown in Fig. 1A). We first discuss the MF approximation, which corresponds to neglecting mRNA-sRNA correlations, and define dimensionless variables that are useful in quantifying deviations between MF results and data from stochastic simulations. To go beyond MF, we use a variational approach which has been successfully applied to gene regulatory networks in recent work [12–15]. Within this approach, we present a general ansatz for the steady-state probability distribution which, at the simplest level, reduces to the MF approximation. At the next level, the variational ansatz gives results that are in excellent agreement with data from simulations for the mean and variance of the regulated mRNA distribution. The proposed method can be used for efficient and accurate quantitative analysis of sRNA-based regulation of gene expression.

We begin by considering the kinetic scheme presented in Fig. 1A. The probability distribution of mRNA and

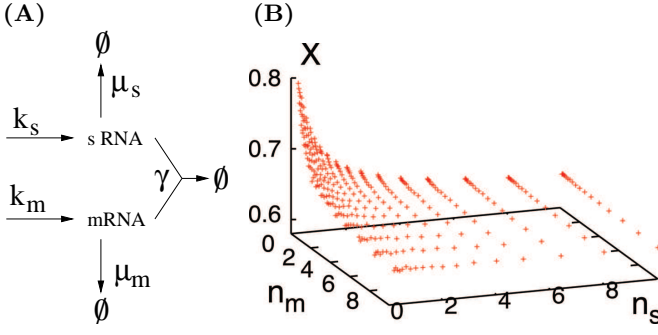


FIG. 1: A) The kinetic scheme for regulation of mRNA by small RNAs with coupled degradation rate γ . B) The ratio $X = \langle m \rangle / n_m$, obtained from simulation data, is plotted as a function of n_m and n_s . Parameters are chosen such that $\epsilon_m = \epsilon_s = 1$ and $\gamma = 1$. For $n_m, n_s \gg 1$, X converges towards the MF production ($X \simeq 0.618$).

sRNA levels per cell, $P_{m,s}(t)$, obeys the master equation:

$$\begin{aligned} \partial_t P_{m,s} = & k_m P_{m-1,s} + k_s P_{m,s-1} \\ & + \mu_m (m+1) P_{m+1,s} + \mu_s (s+1) P_{m,s+1} \\ & + \gamma (m+1)(s+1) P_{m+1,s+1} \\ & - (k_m + k_s + \mu_m m + \mu_s s + \gamma m s) P_{m,s}, \end{aligned} \quad (1)$$

where k_j , μ_j ($j = m, s$) and γ are the parameters defined in Fig. 1A. We will focus on the stationary distribution, denoted by $P_{m,s}^*$. It is convenient to define the following set of independent dimensionless parameters: $\epsilon_m = k_s \gamma / \mu_m \mu_s$, $\epsilon_s = k_m \gamma / \mu_m \mu_s$ and $n_j = k_j / \mu_j$ ($j = m, s$). From the master equation (1), we can explicitly relate the average mRNA and sRNA levels to the correlation term $\langle ms \rangle$ [16, 17] via:

$$\frac{1}{\epsilon_m} \left(1 - \frac{\langle m \rangle}{n_m} \right) = \frac{1}{\epsilon_s} \left(1 - \frac{\langle s \rangle}{n_s} \right) = \frac{\langle ms \rangle}{n_m n_s}, \quad (2)$$

where $\langle \cdot \rangle$ denotes the stationary average. More generally, moments at one level are coupled to higher-order moments due to the nonlinear interaction term. This hierarchy makes the exact solution of the master equation intractable. Defining $X = \langle m \rangle / n_m$, $Y = \langle s \rangle / n_s$ and $C = \langle ms \rangle / \langle m \rangle \langle s \rangle$, equation (2) leads to

$$\frac{1-X}{\epsilon_m} = \frac{1-Y}{\epsilon_s} = C XY. \quad (3)$$

Traditionally, a first approximation, known as the MF approximation, consists of neglecting correlations through the substitution $\langle ms \rangle \rightarrow \langle m \rangle \langle s \rangle$. The MF assumption thus corresponds to $C = 1$ and leads to

$$\epsilon_m XY + X - 1 = 0, \quad \epsilon_s XY + Y - 1 = 0. \quad (4)$$

Comparing Eqns. (3) and (4), we see that the *exact* means (i.e. solutions of Eqn. (3)) are generated by the

MF solutions considered with the rescaled interaction parameter $\gamma' = C\gamma$. Determination of C can therefore provide accurate estimates of the mean mRNA and sRNA levels. The ratio C is also an indicator of the accuracy of MF: it is a good approximation when $C \simeq 1$, whereas deviations from unity indicate that better approximations are needed.

Furthermore, note that X and Y are, in general, functions of the four parameters ϵ_m , ϵ_s , n_m and n_s ; however the MF approximation (Eq. 4) predicts that both quantities depend only on ϵ_m and ϵ_s . It follows that MF theory breaks down in regions of parameter space where X and Y depend on the parameters n_m and n_s (for fixed ϵ_m and ϵ_s). These regions are indicated by significant deviations between the exact ratio X (Y) and the solution λ_+ (λ_-) of Eq. (4).

We now analyze deviations of the MF results from stochastic simulations data obtained using the Gillespie algorithm [18]. The ratios X and C are plotted in figures 1B and 2A respectively. These data are presented as a function of n_m and n_s , keeping ϵ_m and ϵ_s constant. The figures indicate that both quantities converge towards the MF predictions in the limit $n_s, n_m \gg 1$ ($X \rightarrow 0.618$ and $C \rightarrow 1$). More significantly, the data shows that MF is not a good approximation for small n_m and n_s . This is important to note since, in several cellular systems, mRNA abundances can be low (i.e. n_m is small) [19]. This indicates that more accurate approximation are needed in such cases.

Furthermore, in the uncorrelated approximation, the stationary probability distribution can be written as the product of Poisson distributions $\Pi_{\lambda_+}(m) \times \Pi_{\lambda_-}(s)$, where $\Pi_x(n) = e^{-x} x^n / n!$. Defining the marginal distributions $P_m^* = \sum_s P_{m,s}^*$ and $P_s^* = \sum_m P_{m,s}^*$, the ratio $d_j = \langle j \rangle / (\langle j^2 \rangle - \langle j \rangle^2)$ ($j = m, s$) measures deviations between the marginals (P_j^*) and the simple Poisson distribution. Again, deviations of $D = d_s \times d_m$ from unity reveal that both marginal probability distributions cannot be approximated by the Poisson distribution. In Fig. 2B, stochastic simulations data indicate that the coefficient D deviates significantly from one for large n_m and n_s . This observation implies that higher-order terms, such as $\langle m^2 \rangle$ and $\langle s^2 \rangle$ cannot be obtained using the MF prediction $\langle j^2 \rangle - \langle j \rangle^2 = \langle j \rangle$ ($j = m, s$), even in regions of parameter space for which the mean values are given accurately by the MF approximation. Interestingly, it is for small parameter values n_j ($j = m, s$), for which the MF approximation does not give accurate mean values, that D converges to one. This observation is an indication that the Poisson distribution is in some way embedded in the structure of $P_{m,s}^*$.

Based on the preceding analysis, it seems natural to approximate $P_{m,s}^*$ as a superposition of Poisson distributions. This approximation can be implemented using the variational method introduced by Eyink [20], combined with the quantum Hamiltonian formalism of the master

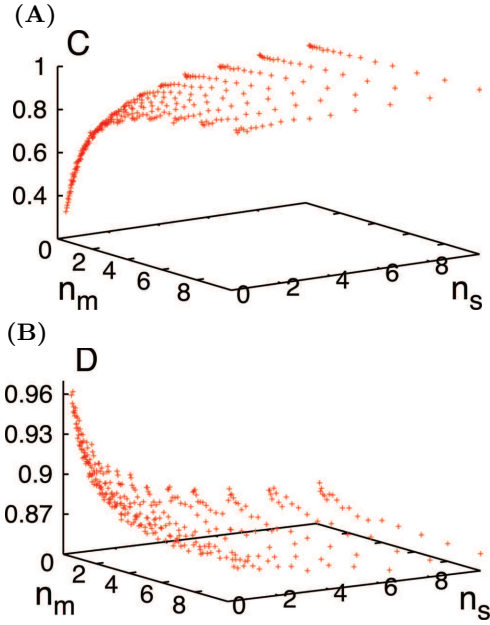


FIG. 2: Stationary value of $C = \langle ms \rangle / \langle m \rangle \langle s \rangle$ (A) and $D = d_m \times d_s$ (B), obtained from simulation data, plotted as a function of n_m and n_s . We keep $\epsilon_m = \epsilon_s = 1$ and $\gamma = 1$.

equation [12, 13]. Following the mapping outlined by Doi [21], we define the operators a^\dagger and a (respectively b^\dagger and b) associated with the creation and annihilation of mRNA (sRNA). The master equation (1) takes the compact form $\partial_t |\psi(t)\rangle = -\mathcal{L}|\psi(t)\rangle$ with

$$\begin{aligned} \mathcal{L} = & k_m + k_s + \mu_m a^\dagger a + \mu_s b^\dagger b + \gamma a^\dagger a b^\dagger b \\ & - (k_m a^\dagger + k_s b^\dagger + \mu_m a + \mu_s b + \gamma ab), \end{aligned} \quad (5)$$

where $[a, a^\dagger] = [b, b^\dagger] = 1$ and $a|0, s\rangle = 0$, $b|m, 0\rangle = 0$. Focusing on the stationary state, we denote by $\langle \psi_L |$ and $|\psi_R\rangle$ the left and right eigenstates with vanishing eigenvalue. They obey $\langle \psi_L | n, m \rangle = \langle \psi_L | \psi_R \rangle = 1$. The mapping to the original problem is given by $P_{m,s}^* = \langle m, s | \psi_R \rangle / m! s!$.

To initiate the variational ansatz, we define the left and right trial vectors ($\langle \phi_L(\Lambda_L) |$ and $|\phi_R(\Lambda_R)\rangle$), constructed using a set of independent parameters, Λ_L and Λ_R . Defining the functional $\mathcal{H}(\Lambda_L, \Lambda_R) = \langle \phi_L | \mathcal{L} | \phi_R \rangle$, the eigenstates are determined using the variational principle $\delta \mathcal{H} = 0$. A detailed explanation of the variational scheme is provided in [20].

We now generalize the uncorrelated approximation to propose a specific ansatz for the trial vectors as the superposition of Poisson distributions. A similar ansatz has also been proposed in a recent study of reaction systems including different chemical species [15]. We define

$$|\phi_L(\Lambda_L)\rangle = \langle 0, 0 | e^{a+b} \prod_{i,j=0}^d e^{\theta_{i,j} a^i b^j}, \quad (6)$$

$$|\phi_R(\Lambda_R)\rangle = \sum_{i,j=1}^d \Theta_{i,j} e^{\alpha_i (a^\dagger - 1)} e^{\beta_j (b^\dagger - 1)} |0, 0\rangle, \quad (7)$$

with $\Lambda_R = \{\alpha_p, \beta_q, \Theta_{p,q}\}$ and $\Lambda_L = \{\theta_{p,q}\}$ ($\theta_{d,d} = 0$). In each vector, the total number of parameters \mathcal{N} is given by $\mathcal{N} = d(d+2)$. The parameters of $\langle \phi_L |$ are imposed by the condition $\langle \phi_L | m, n \rangle = 1$ which leads to $\theta_{p,q} = 0, \forall p, q$. It follows that the set Λ_R is solution of $\langle \delta \phi_L | \mathcal{L} | \phi_R \rangle |_{\Lambda_L = \{0\}} = 0$. Our calculation leads to the system of equations:

$$\begin{aligned} \sum_{p,q=1}^d \Theta_{p,q} \alpha_p^i \beta_q^j \times [\epsilon_s \epsilon_m (ij + i\beta_q + j\alpha_p) \\ + i n_s \epsilon_s (1 - n_m / \alpha_p) + j n_m \epsilon_m (1 - n_s / \beta_q)] = 0, \end{aligned} \quad (8)$$

generated for $i, j = 0, 1, 2, \dots, d$ with the pair ($i = d, j = d$) excluded. The first equation (for $i = j = 0$), corresponds to the probabilistic interpretation: $\langle \phi_L | \phi_R \rangle = 1$ and leads to the normalization constraint $\sum_{p,q} \Theta_{p,q} = 1$. From equation (8) one can then generate the \mathcal{N} independent conditions required to determine the right eigenvector parameters. It follows that an approximation of the stationary distribution is given by $\mathcal{P}_{m,s}^* = \langle m, s | \phi_R(\Lambda_R^*) \rangle / m! s!$, where $\Lambda_R^* = \{\alpha_p^*, \beta_q^*, \Theta_{p,q}^*\}$ is solution of (8). The latter distribution can be explicitly written as a superposition of Poisson distributions: $\mathcal{P}_{m,s}^* = \sum_{p,q} \Theta_{p,q}^* \Pi_{\alpha_p^*}(m) \Pi_{\beta_q^*}(s)$. We note that the MF results are recovered by considering the ansatz with $d = 1$. In this case, $\mathcal{P}_{m,s}^*$ is simply a product of two Poisson distributions with means α and β respectively. The variational equations give $n_s(n_m - \alpha) - \epsilon_m \alpha \beta = 0$ and $n_m(n_s - \beta) - \epsilon_m \alpha \beta = 0$, leading to $X = \lambda_+$ ($Y = \lambda_-$) and $C = D = 1$.

Going one step beyond the MF approximation, we consider the ansatz (7) with $d = 2$. We first consider the symmetric case $k_m = k_s = k$ and $\mu_m = \mu_s = \mu$. This choice imposes $\alpha_j = \beta_j$ ($j = 1, 2$) and $\Theta_{1,2} = \Theta_{2,1}$. The set Λ_R^* , solution of the equations generated by (8), is obtained numerically using standard routines. From a practical point of view, the numerical calculation is significantly faster than stochastic simulations, especially if we need to explore large regions of parameter space.

Figure 3A presents a comparison of our results with data from stochastic simulations. Keeping the ratios ϵ_m and ϵ_s constant, the quantities X , C and D are plotted as a function of μ for $\gamma = 1, 5$ and $\gamma = 10$. Clearly, deviations from MF results appear more pronounced as γ increases. However, for a range of parameter values μ and even for large mRNA-sRNA coupling, the variational scheme gives accurate values of the mean mRNA level per cell ($\langle m \rangle = X \times n_m$). Additionally, we checked that the predictions for $\langle s \rangle$ also presents an excellent agreement with simulation data. Importantly, the agreement of our predictions with simulation data, for the quantities C and D , shows that the variational method also gives accurate values of higher order terms such as the correlation $\langle ms \rangle$ ($= C \times \langle m \rangle \langle s \rangle$) and variance $\langle j^2 \rangle - \langle j \rangle^2$ ($= \langle j \rangle / d_j$).

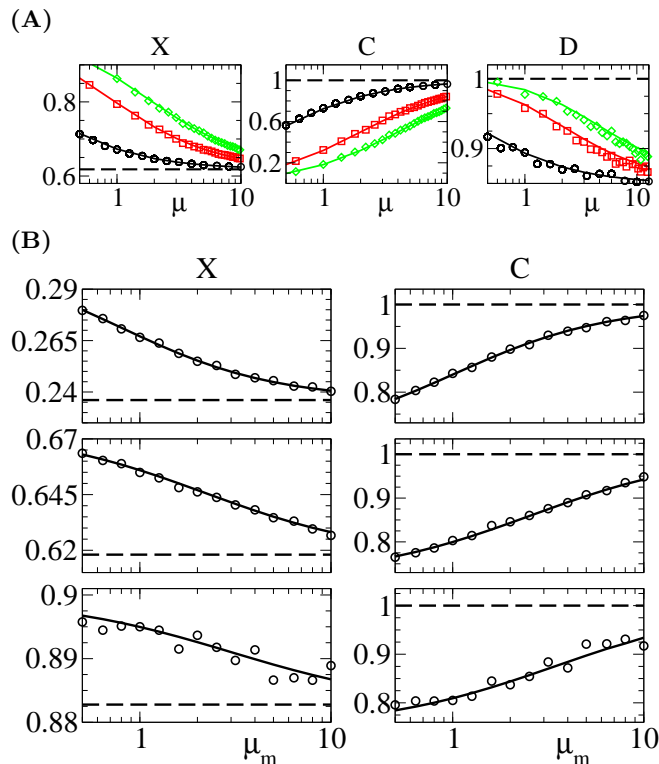


FIG. 3: Comparisons of simulation data (symbols), ansatz predictions (lines) and MF results (dashed line). (A) The quantities $X = \langle m \rangle / n_m$, $C = \langle ms \rangle / \langle m \rangle \langle s \rangle$ and $D = d_s \times d_m$ are plotted as a function of $\mu = \mu_m = \mu_s$ on a logarithmic scale, for $\gamma = 1$ (circles), $\gamma = 5$ (squares), and $\gamma = 10$ (diamonds). We keep $\epsilon_m = \epsilon_s = 1$ with $k_m = k_s = k$. (B) The quantities X (left) and C (right) are plotted as a function of μ_m on a logarithmic scale, for $\epsilon_m = 4$ (top), $\epsilon_m = 1$ (middle) and $\epsilon_m = 1/4$ (bottom). We keep $\mu_s = 2$, $\gamma = 1$ and $\epsilon_s = 1$.

To compare our results in the non-symmetric case, we consider variations in μ_m , keeping $\mu_s = 2$ and $\gamma = 1$ fixed. The set of parameters is once again computed numerically, solving 8 coupled equations generated from equation (8). The ratio ϵ_s is kept equal to unity while $\epsilon_m = 4, 1$ and $1/4$. As shown in Fig. 3B, the ansatz predictions are, once again, in excellent agreement with simulation data.

In conclusion, we have presented a variational approach for analyzing a coupled degradation mechanism of sRNA-based regulation. The latter method generates a set of algebraic equations that can be solved numerically. At the simplest level, the approach reduced to the MF approximation which is shown to be inaccurate for low abundances of the interacting components. The approach proposed allows for systematic improvements over MF and, at the next level, gives excellent agreement with simulation data for the mean and variance of steady-state mRNA/sRNA distributions. The results derived will aid approaches for inference of model parameters from exper-

imental measurements of mean and variance. More generally, the proposed approach can be extended to treat other biological networks with nonlinear interactions for which analytical solutions of the corresponding stochastic models are intractable. In such cases, the proposed procedure of constructing the variational ansatz (i.e. superposition of MF probability distributions) can lead to accurate estimates of the mean and variance for quantities of interest. It is hoped that future work coupling such approaches with experiments will lead to quantitative understanding of gene expression in complex networks.

We would like to thank the Stat. Mech. and NDSSL groups at Virginia Tech, especially professor S. Eubank. This research is funded by the US National Science Foundation through PHY-0957430, DMR-0705152 and the NIH MIDAS project 2U01GM070694-7.

* Electronic address: platini@vbi.vt.edu

† Electronic address: tjia@vt.edu

‡ Electronic address: kulkarni@vt.edu

- [1] S. Gottesman, Trends Genet. **21**, 399 (2005).
- [2] M. Inui, G. Martello, and S. Piccolo, Nat. Rev. Mol. Cell Biol. **11**, 252 (2010).
- [3] E. Hornstein and N. Shomron, Nat. Genet. **38**, S20 (2006).
- [4] A. Raj and A. van Oudenaarden, Ann. Rev. Biophys. **38**, 255 (2009).
- [5] E. Masse, F. Escorcía, and S. Gottesman, Genes & Development **17**, 2374 (2003).
- [6] E. Levine and T. Hwa, Curr Opin in Microbiol **11**, 574 (2008).
- [7] E. Levine, Z. Zhang, T. Kuhlman, and T. Hwa, PLoS Biol **5**, e229 (2007).
- [8] N. Mitarai, A. M. Andersson, S. Krishna, S. Semsey, and K. Sneppen, Phys Biol **4**, 164 (2007).
- [9] P. Mehta, S. Goyal, and N. S. Wingreen, Mol Sys Biol **4** (2008).
- [10] V. P. Zhdanov, Biosystems **95**, 75 (2009).
- [11] Y. Shimoni, G. Friedlander, G. Hetzroni, G. Niv, S. Altuvia, O. Biham, and H. Margalit, Mol. Sys. Biol. **3** (2007).
- [12] M. Sasai and P. G. Wolynes, Proc Natl Acad Sci USA **100**, 2374 (2003).
- [13] Y. Lan, P. G. Wolynes, and G. A. Papoian, J Chem Phys **125**, 124106 (2006).
- [14] J. Ohkubo, J. Stat. Mech. **2007**, P09017 (2007).
- [15] J. Ohkubo, Journal of Chemical Physics **129** (2008).
- [16] V. Elgart, T. Jia, and R. V. Kulkarni, Biophys. J. **98**, 2780 (2010).
- [17] E. Levine, M. Huang, Y. M. Huang, T. Kuhlman, H. Shi, Z. Zhang, and T. Hwa (2010), (*Proc. Natl. Acad. Sci. USA, in submission*).
- [18] D. T. Gillespie, J. Phys. Chem. **81**, 2340 (1977).
- [19] S. Kar, W. T. Baumann, M. R. Paul, and J. J. Tyson, Proc. Natl. Acad. Sci. USA **106**, 6471 (2009).
- [20] G. Eyink, Phys. Rev. E **54**, 3419 (1996).
- [21] M. Doi, J. Phys. A **9**, 1465 (1976).